Lithos 119 (2010) 289–296

Contents lists available at ScienceDirect

Lithos

journal homepage: www.elsevier.com/locate/lithos

Rapid development of the great Millennium eruption of Changbaishan (Tianchi) Volcano, China/North Korea: Evidence from U–Th zircon dating

Haibo Zou [a,*], Qicheng Fan [b], Hongfu Zhang [c]

[a] Department of Geology and Geography, Auburn University, Auburn, AL 36849, USA
[b] Institute of Geology, China Earthquake Administration, Beijing 100029, China
[c] State Key Laboratory of Lithospheric Evolution, Institute of Geology and Geophysics, Chinese Academy of Sciences, Beijing 100029, China

ARTICLE INFO

Article history:
Received 29 January 2010
Accepted 9 July 2010
Available online 3 August 2010

Keywords:
Zircon
Changbaishan Volcano
Eruption
Rhyolite
Magma storage time

ABSTRACT

The Changbaishan (Tianchi) volcano extending across the border of northeast China and North Korea erupted ~100 km^3 peralkaline rhyolites around 1000 AD. This Millennium eruption of the Changbaishan volcano is one of the two largest explosive eruptions in the past 2000 years. Here we report the results of uranium–thorium dating of zircons from the Changbaishan volcanic rocks. Our data indicate that the rhyolitic magmas were stored in the crust for only 8.2 ± 1.2 ka prior to eruption. Based on titanium-in-zircon geothermometer and alkali feldspar-glass geothermometer, the rhyolitic magmas were formed at a relatively low temperature (~740 ± 40 °C). This storage time is very short compared with other large volume catastrophic silicic eruptions. This work demonstrates that peralkaline rhyolitic magmas from the Changbaishan volcano can develop into a catastrophic eruptive phase quite quickly.

1. Introduction

Huge explosive volcanic eruptions probably present the ultimate natural hazard to mankind (Self and Blake, 2008), yet our understanding of such catastrophic eruptions is relatively incomplete. The great Changbaishan eruption in about 1000 AD represents one of the two largest explosive eruptions in the past 2000 years (Dunlap et al., 1992; Liu et al., 1998; Horn and Schmincke, 2000). The Changbaishan volcano (also named Tianchi, Baitoushan, Baegdusan or Paektusan volcano) extends over the border of northeast China and North Korea (E 128°, N 42°) (Fig. 1). ^{14}C ages of charred wood buried by the eruption range from 935 AD to 1024 AD (Dunlap et al., 1992; Horn and Schmincke, 2000; Nakamura et al., 2007; Wei et al., 2007). This huge eruption of Changbaishan volcano ejected about 100 km^3 of tephra and is known as the 'Millennium eruption.' The Changbaishan Millennium eruption with a Volcanic Explosivity Index (VEI) of 7, is comparable in magnitude to the great Tambora eruption of 1815 AD (Indonesia) (Sigurdsson and Carey, 1989; Self et al., 2004; Miller and Wark, 2008). On a global scale, magnitude 7 volcanic eruptions may have taken place five times in the Holocene (the past 10,000 years) (Siebert and Simkin, 2002) with an average frequency of one every 2000 years; however, the global average frequency does not necessarily represent the real likelihood of an eruption for a particular volcano or in a particular region.

Changbaishan is a 2744 m tall conical stratovolcano with a caldera. The volcano sits on the Gaima plateau, a 2–5 Ma, 15,000 km^2 trachybasalt shield which is underlain by Archean–Proterozoic metamorphic rocks of the North China–Korean Craton. The cone of the Changbaishan volcano is composed of younger (<1.0 Ma) trachyte, much of which was removed during the Millennium eruption. The collapse of the upper cone into the emptied magma chamber during this eruption also produced a 5 km wide caldera (Machida and Arai, 1983; Dunlap et al., 1992; Liu et al., 1998; Wei et al., 2003). The caldera now contains a 384 m deep lake named Tianchi (heaven lake). Formation of the Changbaishan volcano and other dispersed volcanoes in northeast China is related to the upwelling of the hot asthenosphere in the mantle wedge above the stagnant Pacific slab (Lei and Zhao, 2005; Zou et al., 2008; Zhao et al., 2009a). It appears that decompression melting associated with the upwelling plays a dominant role in melt generation and slab fluid contribution is minimal or absent (Zou et al., 2003; Chen et al., 2007; Zou et al., 2008).

The Millennium eruption mainly produced rhyolitic pumice and ash. The fallout fan from the Plinian and co-ignimbrite ash extends as far as north Japan, ~1200 km (Fig. 1). The rhyolitic pumice formed by pyroclastic flows extends more than 70 km from the crater. The thickness of the rhyolitic pumice varies from 70 m near the Tianchi caldera (e.g., Baiyanfeng or Baiyan Peak), to 0.7 m in Yuanchi (32 km from the caldera), to 0.12 m in east Diaoyutai, North Korea (65 km from the caldera).

The Changbaishan rhyolites contain 71–73 wt.% SiO_2, 10.4–11.5 wt.% Al_2O_3, 0–0.36 wt.% MgO, 0.04–0.6 wt.% CaO, and high total alkali contents ($Na_2O + K_2O$) (Fig. 2). Their ($Na_2O + K_2O$)/Al_2O_3 molar ratios

* Corresponding author. Tel.: +1 334 844 4315.
E-mail addresses: haibo.zou@gmail.com, haibo.zou@auburn.edu (H. Zou).

0024-4937/$ – see front matter
doi:10.1016/j.lithos.2010.07.006

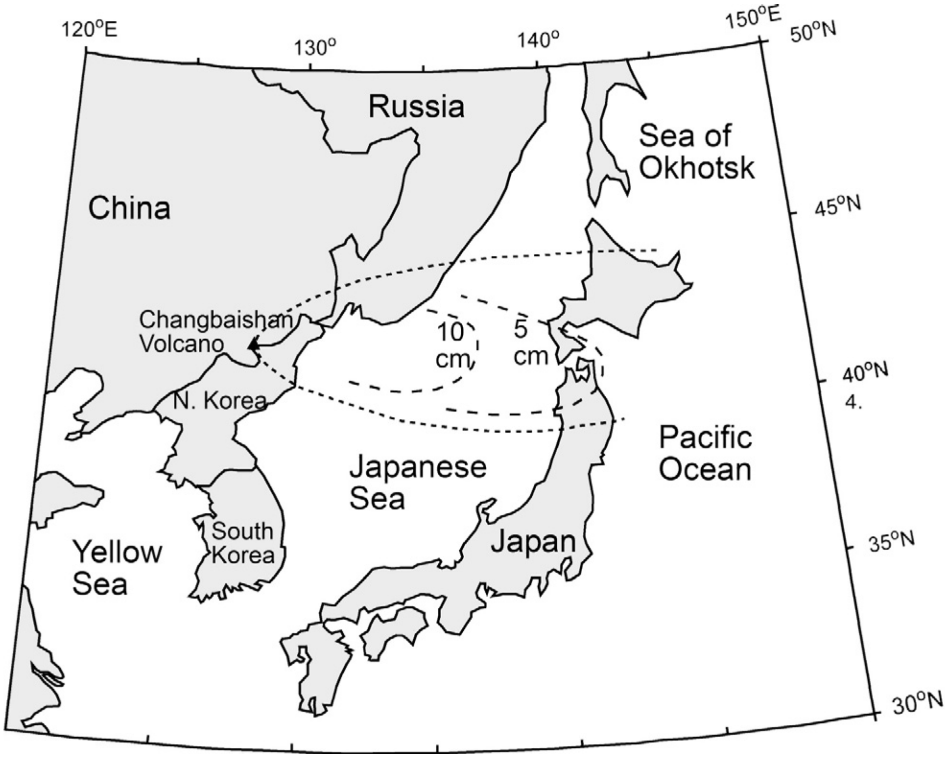

Fig. 1. Locality of the Changbaishan volcano and the distribution of tephras from the Changbaishan volcano. Revised from Machida and Arai (1983).

range from 1.09 to 1.30, indicating that these peralkaline rhyolites are comendites. The comendites are 30% vesicular and contain 2% crystals, 90% of which are alkali feldspar, with quartz is a minor phase. The Changbaishan Millennium eruption represents a rare occurrence of a large explosive eruption of peralkaline rhyolitic rocks in historic times.

The main aim of this work is to constrain the timescales and dynamics of rhyolitic magma storage in the crust, by dating newly observed zircon ($ZrSiO_4$) crystals in these rhyolitic rocks using short-lived uranium–thorium (U–Th) isotope disequilibrium. The small uncertainty in very young eruption ages ($1^{+0.02}_{-0.08}$ ka) is helpful for determining magma storage time. In addition we estimate the magma temperature using Ti-in-zircon geothermometry and alkali feldspar-glass geothermometry.

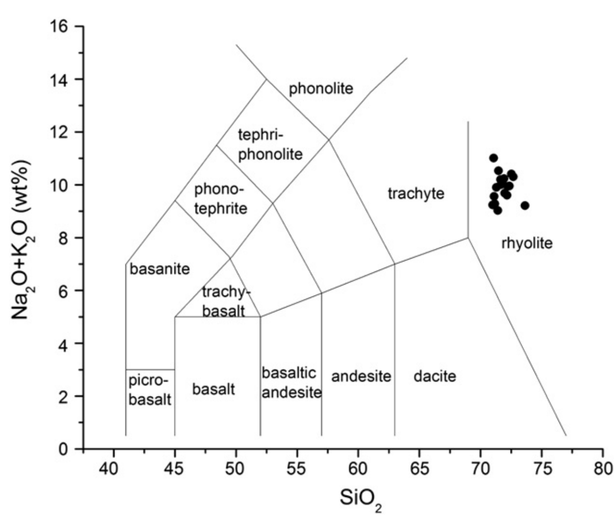

Fig. 2. Total alkali vs. silica (TAS) plot (Le Bas et al., 1986) for the Millennium rhyolites from Changbaishan.
Data sources (Liu et al., 1998; Fan et al., 2006; Wei et al., 2006; Zou et al., 2008).

2. Ion probe and electron probe methods

Zircon grains were pressed in indium metals, polished and coated with gold. U–Th isotope disequilibrium dating was performed on individual zircon crystals using the UCLA CAMECA ims 1270 secondary ion mass spectrometer (ion microprobe). Analytical techniques for U–Th isotopes have been documented in Reid et al. (1997), Schmitt (2006) and Zou et al. (2010). Ion microprobe ($^{230}Th/^{232}Th$) and ($^{238}U/^{232}Th$) analyses with the CAMECA ims 1270 routinely achieve a relative precision and accuracy of ~1–2% with a spot size of ~25 μm diameter and a depth resolution of <3 μm in single electron multiplier collector peak-jumping mode. A 35 to 45 nA mass-filtered $^{16}O^-$ beam was focused into a ~25 μm diameter oval spot. Secondary ions were accelerated at 10 keV with an energy bandpass of 50 eV and analyzed at a mass resolution of 5000. Relative sensitivities for ^{238}UO and ^{232}ThO were calibrated by measuring the radiogenic $^{206}Pb/^{208}Pb$ ratio of concordant reference zircons AS-3 and 91,500 (Paces and Miller, 1993; Wiedenbeck et al., 1995). Absolute ages can be calculated by isochron regression if the spread in U/Th is sufficiently large and mean square weighted deviation (MSWD) is small (<2.5). Alternatively, if the data points are scattered, then two-point isochron model ages can be calculated from SIMS zircon spot analyses and bulk glass (or whole-rock) isotope compositions with age uncertainties for individual zircons.

Analytical procedures for Ti concentrations in zircons using ion probe followed those documented in literature (Monteleone et al., 2007; Schmitt et al., 2010). Species of $^{48}Ti^+$ and $^{30}Si^{16}O^+$ were measured in each cycle. Ti/Si relative sensitivity factor were calibrated on SL-13 zircons with a Ti abundance of 6.32 ppm (Harrison et al., 2007). During Ti concentration analysis, $^{56}Fe^{28}Si^{16}O^{2+}$ were monitored to detect beam overlap over mineral inclusions. Only one zircon grain (grain 2 from Yuanchi) had high $^{56}Fe^{28}Si^{16}O^{2+}$ intensity, and Ti concentration for grain 2 from Yuanchi was discarded (Table 1).

Feldspar and glass compositions were analyzed by JEOL JXA-8100 electron probe in State Key Laboratory of Lithospheric Evolution,

Table 1
Zircon U–Th isotope and Ti concentration data. U and Th isotope activity ratios and titanium concentrations in zircons.

	Grain #	($^{238}U/^{232}Th$)	1σ	($^{230}Th/^{232}Th$)	1 σ	Ti* (ppm)	T (°C) $\alpha_{TiO2}=0.5$	T (°C) $\alpha_{TiO2}=0.34$
Baiyangfeng								
Zircon	1	5.332	0.114	1.144	0.077	3.0	701	735
Zircon	2	4.474	0.096	1.012	0.089	1.8	657	689
Zircon	3	4.542	0.097	1.019	0.084	2.8	693	726
Zircon	4	3.105	0.071	0.986	0.047	3.1	702	736
Zircon	5	4.795	0.103	1.142	0.084	4.2	730	767
Zircon	6	4.671	0.100	1.033	0.088	3.0	701	736
Zircon	7	3.003	0.072	0.877	0.044	5.0	746	783
Zircon	8	3.813	0.082	1.053	0.054	1.9	662	694
Zircon	9	4.328	0.093	1.033	0.082	3.6	715	750
Zircon	10	4.333	0.097	1.142	0.076	2.5	685	718
Zircon	11	3.182	0.068	0.908	0.104	4.4	734	770
Yuanchi								
Zircon	1	5.329	0.127	1.112	0.110	1.8	658	689
Zircon	2	5.576	0.119	1.004	0.073	**		
Zircon	3	5.112	0.114	1.178	0.088	3.9	722	758
Zircon	4	3.625	0.080	0.870	0.054	3.6	716	752
Zircon	5	4.216	0.090	0.980	0.066	5.7	759	797
Zircon	6	4.010	0.087	0.845	0.078	3.4	711	746
Zircon	7	4.962	0.106	0.882	0.088	1.5	644	674
Ave. T (°C)							702	736
1 S.D. T (°C)							33	35

*Overall accuracy and precision of the Ti concentration are 5 to 10% (2 SD) for a single Ti analysis.
**Ti concentration is not reported due to the presence of a Ti-bearing inclusion in this Ti measurement spot.

Institute of Geology and Geophysics, Chinese Academy of Sciences. Analytical methods for major elements have been documented in literature (e.g., Su et al., 2009; Zhao et al., 2009b). Analytical conditions are 15 kV accelerating voltage and 10 nA beam current. Beam diameters were 10 microns for glass analysis and 5 to 8 microns for feldspar analysis.

3. Samples and results

Two peralkaline rhyolitic pumice samples produced by the Millennium eruption were collected from Baiyanfeng on the edge of the Tianchi caldera, and from Yuanchi at 32 km to the east of the Tianchi caldera, respectively. Crystals are rare in rhyolitic pumices (2%) and are mainly composed of anorthoclase. We identified 11 zircon grains from Baiyanfeng rhyolitic pumice and 7 zircon grains from Yuanchi rhyolitic pumice. Representative images of zircons from Baiyanfeng and Yuanchi are provided in Fig. 3. The 18 individual zircons are analyzed for U–Th isotopes and titanium concentrations.

The 11 zircon grains from Baiyanfeng and whole-rock pumice yield a high-quality U–Th isochron age of 10.6 +1.6/−1.5 thousand years (ka) (2σ error) (Fig. 4), with mean squared weighted deviates (MSWD) of 0.61. The 7 zircon grains from Yuanchi yield a U–Th isochron age of 7.3 +1.8/−1.7 (2σ) (Fig. 5), with a MSWD of 1.4. Although the zircon isochron age from Baiyanfeng appears to be slightly older than that of Yuanchi, their ages are close to the measurement uncertainties. When all the 18 grains are considered together, the isochron age is 9.2±1.2 ka, with MSWD of 1.4 (Fig. 6). These zircons represent some of the youngest zircons that have been dated by well-defined U–Th isochrons (excluding two-point isochrons) in literature. Since our U–Th isotope data points are not scattered, it is not necessary to use individual two-point model ages.

All zircons have low Ti concentrations, ranging from 1.8 to 5.0 ppm for Baiyanfeng zircons, and from 1.5 to 5.7 ppm for Yuanchi zircons (Table 1).

Feldspar and glass compositions measured by electron probe are presented in Table 2. The compositions of feldspars in comendites span a very limited range. Average feldspar composition from Baiyanfeng pumice is $Or_{37}Ab_{62.6}An_1$, and average feldspar composition from Yuanchi pumice is $Or_{33.7}Ab_{65.3}An_{0.1}$. Thus all feldspars are alkali feldspars with low An (<1%). Glass compositions from Baiyanfeng and Yuanchi are also similar and are enriched in SiO_2 (74%), Na_2O (5%) and K_2O (4%).

4. Discussion

4.1. Fractional crystallization vs. crustal melting

Rhyolitic magmas may be produced by fractional crystallization of trachytic magmas or by melting of pre-existing silicic crustal rocks. Our U–Th zircon data and available trace element data can be used to evaluate the models.

U–Th isotope zircon dating has not detected any old zircon grains or cores in the rhyolitic pumice. The 9 ka zircons therefore do not come from the Archean–Proterozoic metamorphic rocks in the North China–Korean Craton or from Mesozoic granites in NE China. Furthermore, there are no xenoliths of crustal material in the Changbaishan rhyolites. Although absence of evidence of old zircons is not evidence of absence, the contribution, if any, of pre-existing crustal rocks is minor. Additional evidence against crust melting as the origin of the Changbaishan rhyolites comes from the Nd isotopic compositions and Sr concentrations of the rhyolitic pumice. Changbaishan rhyolites and trachytes have similar Nd isotope compositions ($^{143}Nd/^{144}Nd$ values are 0.512586 for trachytes and 0.512582 for rhyolites) (Zou et al., 2008). The rhyolitic pumices have 297–350 ppm Rb, 5.0 to 6.9 ppm Sr and Rb/Sr ratios ranging from 43.4 to 69.4 (Basu et al., 1991; Zou et al., 2008). As crustal rocks are enriched in Sr (~600 ppm), partial melting of common crustal rocks is unlikely to generate rhyolitic magmas with very low Sr concentrations (5.0 to 6.9 ppm) and high Rb/Sr (43 to 69). A quartz-rich crustal rock would have low Sr, but such a rock may not have high Rb/Sr ratios. Although we cannot completely rule out the possibility of a quartz-rich crustal rock, the most likely way to produce rhyolites with very low Sr contents is by fractional crystallization of feldspars in a magma chamber (Mahood, 1990; Halliday et al., 1991), as Sr strongly partitions into feldspars during fractional crystallization of rhyolitic magmas.

To sum up, the nearly identical Nd isotopic compositions between trachytes (0.512586) and rhyolites (0.512582), the very low Sr concentrations in rhyolites, as well as the lack of inherited zircons also indicate that rhyolitic magmas are produced from fractional

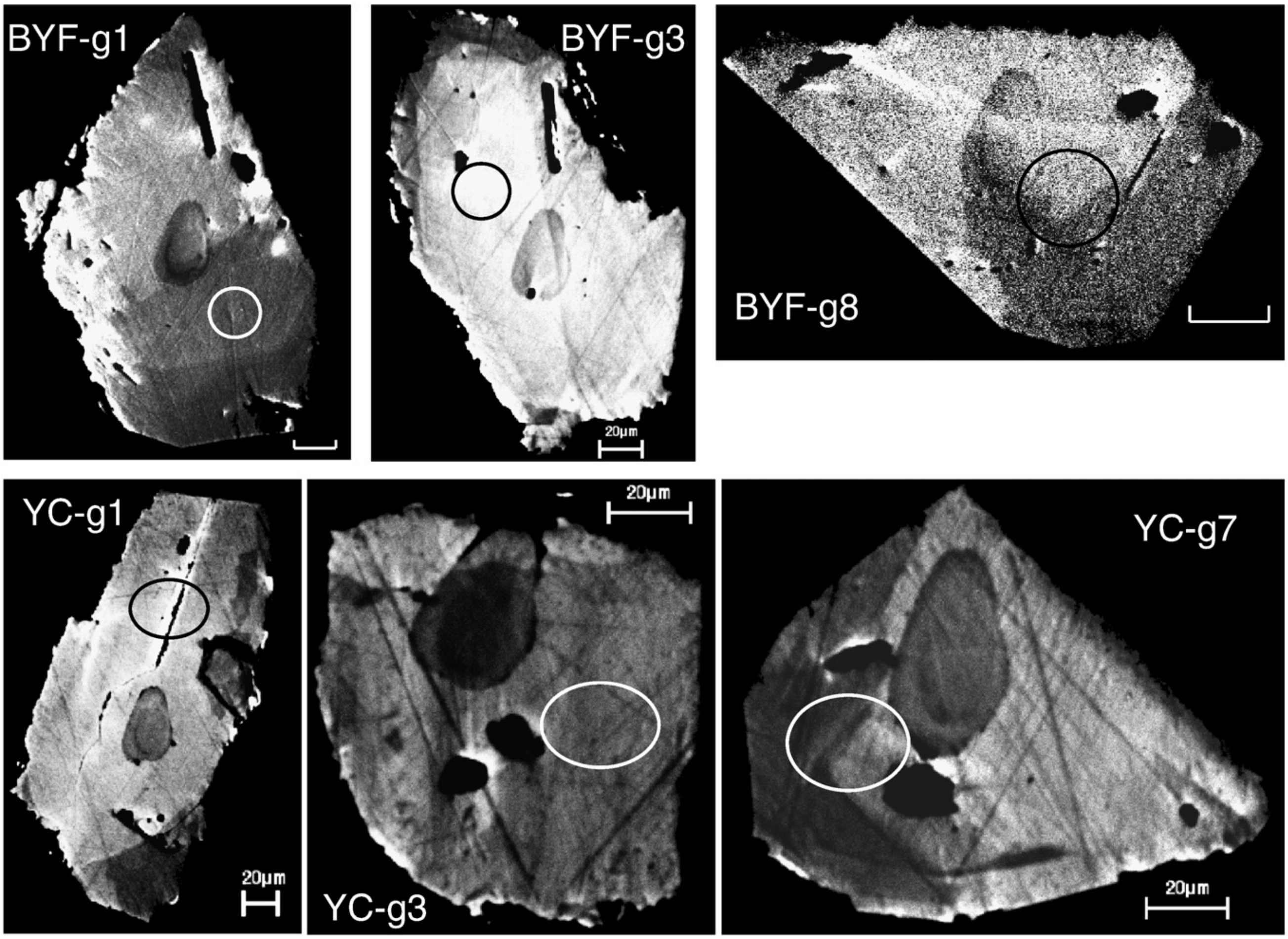

Fig. 3. Selected cathodoluminescence (CL) images of zircons showing SIMS geochronology analysis spots from peralkaline rhyolitic pumices from Baiyanfeng (top panel) and Yuanchi (bottom panel). Black or white ellipses in CL images indicate U–Th spots. Dark beam spots indicate locations of Ti concentration analysis spots. Scale bar in each image is 20 μm. BYF = Baiyanfeng; YC = Yuanchi.

crystallization of feldspars in parental trachytic magmas, rather than melting of pre-existing crustal materials. Thus it is clear the magma chamber was not significantly affected by crustal contamination.

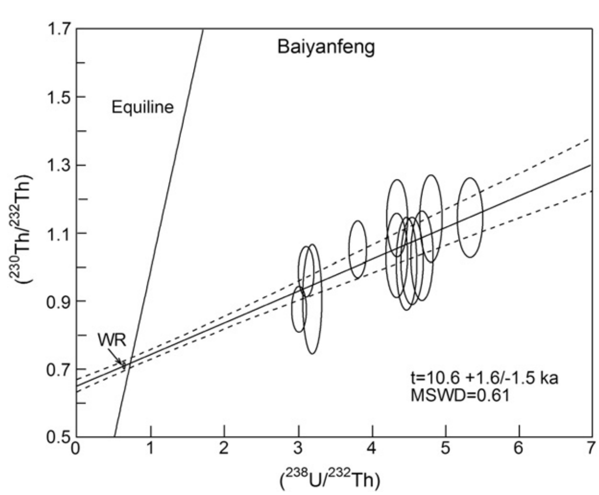

Fig. 4. Uranium–thorium isochron age for 11 zircons from the Baiyanfeng rhyolitic pumice. The zircon ages are calculated from the slope of the regression line (Ludwig, 2003) and the reported age error is 2σ. Error envelopes are also shown. WR = whole rock (the small ellipse). The rhyolitic whole-rock U–Th data are $(^{238}U/^{232}Th) = 0.634 \pm 0.06$, $(^{230}Th/^{232}Th) = 0.711 \pm 0.07$ (Zou et al., 2008).

4.2. Magma storage time

Having established the co-magmatic evolution from trachytes to rhyolites, we can now assess the time scales of magma evolution and storage of rhyolitic magma before the explosive eruption. Since the

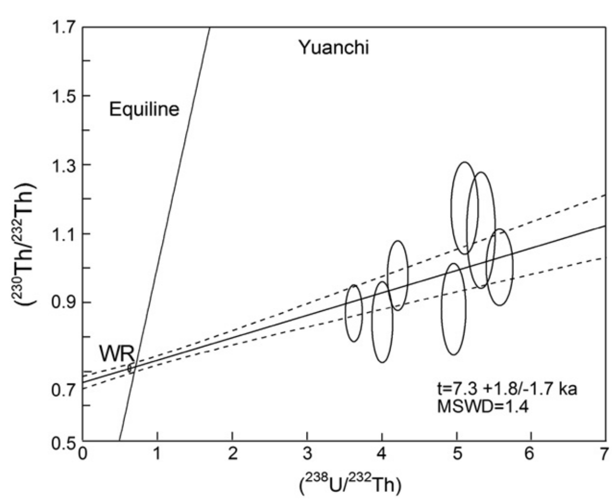

Fig. 5. Uranium–thorium isochron age for 7 zircons from the Yuanchi rhyolitic pumice.

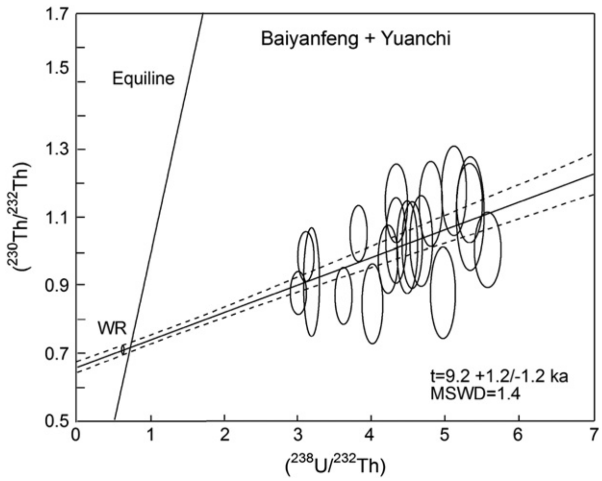

Fig. 6. Uranium–thorium isochron age for all 18 zircons from Baiyanfeng and Yuanchi.

eruption age is 1 ka and the zircon ages are 9.2 ± 1.2 ka, we infer that the zircon residence time in the rhyolitic magma chamber before the Millennium eruption is of the order of 8.2 ± 1.2 ka.

If the analyzed zircons crystallize at the beginning of the formation of the peralkaline rhyolites, then ~8.2 ka is the storage time for the rhyolitic magma in the crust. We recognize however that zircons from some volcanic and plutonic rocks may represent recycled crystals from earlier parental magmas (e.g., Bachmann et al., 2007a; Miller et al., 2007). If the zircons from Changbaishan rhyolitic pumice started to crystallize in the parental trachytic magma, then the rhyolitic magma storage time is shorter than 8.2 ka. In both cases, the conclusion of short storage time for rhyolitic magmas is robust.

The high quality of the U–Th zircon isochron age, the accuracy of the young eruption ages, the low Sr in the Changbaishan rhyolites, and the identical Nd isotopic compositions between rhyolites and trachytes help provide a robust estimate of zircon storage time in the rhyolitic magmas from Changbaishan volcano. The closed-system feature of fractional crystallization helps make the estimate of magma storage time more certain.

The 8.2 ± 1.2 ka storage time for rhyolitic magmas is consistent with a previous approximation from whole-rock uranium–thorium isotope data that the magma evolution time from trachyte to rhyolite is less than 10 ka (Zou et al., 2008). But the previous whole-rock uranium–thorium isotope data do not provide sufficient age resolution owing to small spread in whole-rock U/Th ratios. In comparison, U/Th ratios in zircons often have large spread and are significantly higher than whole rock, permitting good age resolution (Pyle et al., 1988; Condomines, 1997).

Owing to the high viscosity of rhyolitic magmas, rhyolitic magmas are often stored in the magma chamber for a long period of time (Halliday et al., 1989; Reid et al., 1997; Hawkesworth et al., 2004; Turner and Costa, 2007). The magma storage time for rhyolitic magmas can be up to more than several hundred thousand years.

Simon et al. (2008) provide an overview of the zircon pre-eruption ages in young volcanoes. The summary in Simon et al. (2008) includes (1) more than a dozen small volume effusive eruptions with eruption ages ranging from 2170 ka (Pine Mt Gey, Geysers, CA) to 0.6 ka (South Deadman, Long Valley, CA), and (2) a dozen large volume explosive eruptions with eruption ages ranging from 760 ka (Bishop, Long Valley, CA) to 27 ka (Oruanui, New Zealand). Most eruptions in the summary are from multiple eruptions from four localities (Long Valley, Yellowstone, Geysers, and Taupo of New Zealand). U–Th method is used for zircons younger than 300 ka, and U–Pb method is employed for zircons older than 300 ka. Small volume effusive eruptions display a greater range of pre-eruption ages, ranging from 25 ka to >225 ka, whereas large volume explosive eruptions yield a relatively narrow range of pre-eruption ages (50 to 135 ka) (Simon et al., 2008). The pre-eruption zircon ages from Changbaishan (8 ka) are significantly shorter than the reported range for large volume eruptions (50 to 135 ka) (Fig. 7).

4.3. Zircon saturation

The Changbaishan rhyolites are peralkaline rhyolitic melts (comendites). Due to the high Zr solubility in peralkaline melts, zircon saturation level in peralkaline melts is significantly higher than in non-peralkaline melt (e.g., metaluminous melt) (Watson, 1979). Consequently zircon crystals are less common in peralkaline melts. Zircons have been observed in peralkaline rhyolities from Paisano volcano, Trans-pecos Texas (with Zr concentrations of about 1400 ppm), but have not been reported from similar rocks from the African rifts (Parker, 1983). According to the Table 3 in Watson (1979), at least 1000 ppm Zr is needed in a magma to saturate zircons in peralkaline acidic magmas and this is critically dependent on molar $(Na_2O + K_2O)/SiO_2$ ratios and, to a lesser extent, on temperatures and CaO and Fe_2O_3 contents. Since the peralkaline rhyolitic pumices from Changbaishan have Zr concentrations ranging from 1700 to 2600 ppm (Horn and Schmincke, 2000; Fan et al., 2006; Chen et al., 2007; Zou et al., 2008), it is likely that the Changbaishan zircons are saturated (or nearly saturated) with the peralkaline melt. Alternatively, the zircons may have been originally produced from earlier episodes of magmatism, in which case, the peralkaline rhyolitic magma storage time will have been even shorter than the apparent short zircon pre-eruption times (~8 ka).

4.4. Magma temperature

The lack of co-existing 2-pyroxenes, 2-feldspars or Fe–Ti oxides in the rhyolites prevents the use of these conventional geothermometers to determine the magma temperature prior to eruption. As a result we have used the recently developed Ti-in-zircon geothermometry (Watson and Harrison, 2005; Watson et al., 2006) and alkali feldspar-glass geothermometry (Putirka, 2008) to estimate magma temperature.

All the zircons from Baiyanfeng and Yuanchi have relatively low titanium concentrations (1.5–5.7 ppm). The TiO_2 activities in most igneous and metamorphic rocks are generally 0.5 or higher. Typical TiO_2 activities are about 0.6 for rhyolites (Hayden and Watson, 2007). For peralkaline rhyolites, the TiO_2 activity is lower than typical rhyolites. If TiO_2 activity of 0.5 is used, the average temperature for zircon crystallization in Baiyanfeng pumice is 702 ± 28 °C, and the average temperature in Yuanchi pumice is 702 ± 43 °C. Low TiO_2 activity of 0.34 ± 0.11 has been reported for the A-type rhyolites from the Alid Volcanic Center, Eritrea, Northeast Africa (Lowenstein et al., 1997; Hayden and Watson, 2007). If we use 0.34 as TiO_2 activity ratio for Changbaishan, the average temperature increases to 737 ± 30 °C for Baiyanfeng pumice and 736 ± 46 °C for Yuanchi pumice. Their similar zircon ages and temperatures indicate that Baiyanfeng and Yuanchi pumices were derived from the same shallow magma chamber.

Due to the uncertainty in TiO_2 activity and or uncertainty with calibration of the geothermometer (Fu et al., 2008), it is helpful to combine the Ti-in-zircon geothermometer with other geothermometers. Alkali feldspar-glass pair in volcanic rocks can be used to estimate magma temperature. Using the alkali feldspar-glass geothermometer in volcanic rocks (Putirka, 2008), the magma temperature for Baiyanfeng is 741 °C and the temperature for Yuanchi is 752 °C. Typical uncertainties for the alkali feldspar-glass geothermometer are about 30 °C. Temperatures estimated from alkali feldspar-glass geothermometer appear to be slightly higher than those from Ti-in-zircon geothermometer, but both temperature estimates are still within the uncertainties of these two methods. Accordingly, magma temperature is likely to be 740 ± 40 °C. The relatively low temperature is consistent with the high water content

Table 2
Alkali feldspar and glass compositions measured by electron probe.

	BYF feldspar	BYF feldspar	BYF feldspar	BYF feldspar	BYF feldspar	BYF feldspar	BYF glass*	YC feldspar	YC feldspar	YC feldspar
SiO_2	65.63	65.91	65.89	66.58	66.07	65.80	73.52	67.52	67.24	67.13
TiO_2	0.04	0.00	0.05	0.01	0.01	0.06	0.21	0.02	0.00	0.00
Al_2O_3	18.41	18.39	18.53	18.54	18.40	18.44	9.82	18.14	18.06	18.07
FeO	0.24	0.25	0.26	0.28	0.35	0.38	3.91	0.60	0.57	0.52
MnO	0.00	0.00	0.02	0.03	0.02	0.00	0.07	0.00	0.00	0.00
MgO	0.00	0.00	0.01	0.00	0.00	0.02	0.02	0.02	0.00	0.00
CaO	0.17	0.17	0.23	0.18	0.22	0.23	0.21	0.00	0.04	0.02
Na_2O	7.01	7.09	7.17	7.22	7.03	7.10	5.04	7.53	7.52	7.42
K_2O	6.37	6.48	6.33	6.49	6.18	6.41	4.22	5.98	5.78	5.87
Cr_2O_3	0.02	0.00	0.01	0.00	0.02	0.04	0.04	0.02	0.04	0.00
NiO	0.00	0.03	0.00	0.00	0.02	0.00	0.07	0.02	0.00	0.03
Total	97.9	98.3	98.5	99.3	98.3	98.5	97.1	99.8	99.3	99.1
Or	0.371	0.376	0.367	0.373	0.358	0.372		0.341	0.331	0.337
Ab	0.621	0.625	0.631	0.631	0.620	0.626		0.653	0.656	0.648
An	0.008	0.008	0.011	0.009	0.011	0.011		0.000	0.002	0.001
T (°C)***	741	741	742	741	742	740		745	749	750

BYF = Baiyanfeng; YC = Yuanchi.
The temperature estimate is insensitive to pressure change. For example, increasing pressure from 0.3 GPa to 0.4 GPa only increases temperature estimate by 0.1 °C.
* Baiyanfeng glass composition is from Fan et al. (2005) and is used with individual alkali feldspar for calculation of Baiyanfeng magma temperature.
** Average Yuanchi glass composition, along with individual alkali feldspar, is used for the calculation of Yuanchi magma temperature.
*** Temperature is calculated from alkali feldspar-glass pairs using equation 24b for volcanic systems from Putirka (2008). Pressure is assumed 0.3 GPa (about 10 km).

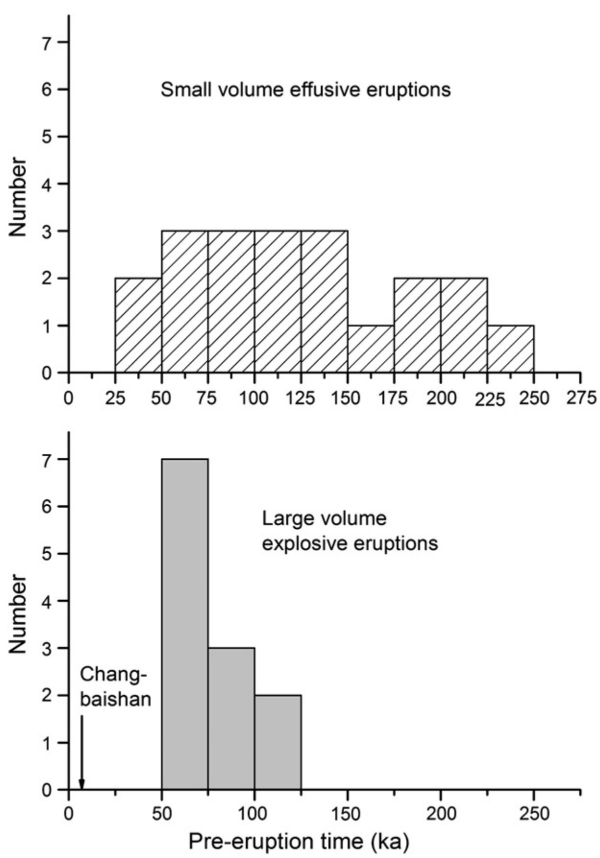

Fig. 7. Histograms for pre-eruption ages for small volume effusive eruptions and large volume explosive eruptions. The data for histogram were compiled by Simon et al. (2008). Dating methods include U–Th zircon ages for young eruptions younger than 160 ka and U–Pb zircon ages for eruptions between 340 ka and 2170 ka (see Table 2 in Simon et al., 2008). Data sources for U–Th and U–Pb zircon ages (Reid et al., 1997; Brown and Fletcher, 1999; Reid and Coath, 2000; Schmitt et al., 2003; Bacon and Lowenstern, 2005; Bachmann et al., 2007a). Eruption ages are mostly obtained by ^{40}Ar–^{39}Ar ages (Pringle et al., 1992; van den Bogaard and Schimick, 1995; Smith et al., 1996; Min et al., 2000; Bachmann et al., 2007b). The apparent pre-eruption age from Changbaishan is indicated with an arrow.

(5 wt.%) (Horn and Schmincke, 2000) in the Changbaishan rhyolitic magma, as rhyolitic magma temperature is inversely related to the magma water content (Scaillet and Macdonald, 2006).

Magma temperature of 780 °C has been estimated for the Changbaishan Millennium eruption (Liu et al., 1998) from physical volcanology, based on the quantitative relationship between solid contents, estimated eruption column height and magma temperature (Sparks, 1986). Although uncertainty levels are not reported by Liu et al. (1998), according to their Fig. 6–13, it appears that the temperature uncertainty is about 100 °C. Thus temperature estimates from Ti-in-zircon geothermometer and alkali feldspar-glass geothermometer and physical volcanology are within the same range. However, compared to physical volcanology, chemical geothermometers used in this study provide temperature estimates with smaller errors.

Phase equilibrium in long-lived silicic magma chambers may eventually trigger explosive volcanic eruptions (Fowler and Spera, 2007). The short storage time (8.2 ± 1.2 ka) of the rhyolitic magma may suggest that the eruption of the rhyolitic magma beneath Changbaishan was not caused by internal phase equilibrium, but by an external trigger. Field studies have observed up to one-meter scale basaltic trachy-andesite blocks in the rhyolitic pumice near the caldera. Basaltic trachy-andesite breccias with 3–7 cm diameter clasts can also be observed in the gray rhyolitic pumices (Liu et al., 1998; Fan et al., 2005). The Millennium eruption may have been triggered by a major injection of a hot and dense basaltic magma body into a cold and light rhyolitic magma chamber (Fan et al., 2005). The temperature of the basaltic magma body would have been ~1000 °C, while the temperature of the rhyolitic magma chamber was ~740 °C as estimated from titanium concentrations in zircons and alkali feldspar-glass geothermometer. This significant temperature contrast between the basaltic magmas and the rhyolitic magmas and the nature of the highly fractionated high volatile (water) rhyolitic magmas in the crust for 8000 years would have made it easier for the injection to trigger the great Millennium eruption.

5. Conclusions

The rhyolitic magma chamber beneath Changbaishan was formed at 9.2 ka BP (before present) by closed-system fractionation of

YC feldspar	YC feldspar	YC feldspar	YC glass	YC glass	YC glass	YC glass	YC glass	YC glass	YC Ave. YC glass**
66.85	67.73	67.03	74.15	72.86	73.17	74.98	72.28	74.31	73.62
0.00	0.00	0.01	0.22	0.21	0.22	0.23	0.19	0.19	0.21
17.82	18.09	18.05	10.10	9.78	9.73	10.03	9.76	9.79	9.87
0.55	0.49	0.46	3.89	3.92	3.94	3.90	3.89	3.89	3.90
0.02	0.00	0.00	0.12	0.06	0.07	0.06	0.08	0.07	0.08
0.00	0.01	0.00	0.01	0.02	0.02	0.01	0.01	0.02	0.01
0.02	0.04	0.02	0.21	0.18	0.21	0.20	0.24	0.20	0.21
7.47	7.59	7.43	5.10	5.10	5.02	5.47	4.61	5.03	5.05
5.94	5.83	5.91	4.16	4.35	4.35	4.19	4.06	4.17	4.21
0.00	0.03	0.02	0.03	0.03	0.05	0.02	0.03	0.06	0.04
0.00	0.02	0.06	0.07	0.00	0.02	0.00	0.04	0.00	0.02
98.7	99.8	99.0	98.1	96.5	96.8	99.1	95.2	97.7	97.23
0.343	0.332	0.340							
0.656	0.658	0.649							
0.001	0.002	0.001							
753	757	758							

parental trachytic magmas, and explosively erupted at 1 ka BP. The magma storage time is about 8 ka, which is significantly short compared with typical residence times of large volume explosive eruptions (50–135 ka). The rhyolitic magmas were at low temperatures (740 °C). Injection of new basaltic magma body into the highly differentiated rhyolitic magma chamber might have triggered the eruption. The short magma storage time and low magma temperature may have helped the Changbaishan large volume rhyolitic magma escape crustal contamination.

Changbaishan volcano is still an active volcano. There is a low seismic velocity zone below Changbaishan volcano extending from 10 to over 65 km depth. An electrical conductivity anomaly exists at 20 km depth below the volcano (Tang et al., 2001). Numerous hot springs and fumaroles are present on the volcano (Shangguan et al., 1997). Although short storage time of 8000 years does not necessarily mean that the next eruption is imminent, our present study does indicate that the still dangerous Changbaishan volcano is capable of rapidly producing catastrophic, explosive eruptions in the foreseeable future.

Acknowledgements

We thank Axel K. Schmitt for assistance with ion probe measurement, Qian Mao for assistance with electron probe measurement, Fu-Yuan Wu, Kevin McKeegan, Simon Turner, Mary Reid, Jim Gill and Jianli Sui for their help. Constructive journal reviews by Asish Basu, Ray Macdonald, and two anonymous reviewers led to significant improvement of this manuscript and are greatly appreciated. Andrew Kerr provided effective handling and editing of the manuscript. The work is supported by National Science Foundation (EAR 0917651), Natural Science Foundation of China (40772038) and Auburn University. The ion probe facility at UCLA is in part supported by NSF Instrumentation and Facility program.

References

Bachmann, O., Charlier, B.L.A., Lowenstern, J.B., 2007a. Zircon crystallization and recycling in the magma chamber of the rhyolitic Kos Plateau Tuff (Aegean arc). Geology 35, 73–76.

Bachmann, O., Oberli, F., Dungan, M.A., Meier, M., Mundil, R., Fisher, H., 2007b. $^{40}Ar/^{39}Ar$ and U–Pb dating of the Fish Cannon magmatic system, San Juan Volcanic field, Colorado: evidence for an extended crystallization history. Chemical Geology 236, 134–166.

Bacon, C.R., Lowenstern, J.B., 2005. Late Pleistocene granodiorite source for recycled zircon and phenocrysts in rhyodacite lava at Crater Lake, Oregon. Earth and Planetary Science Letters 233, 277–293.

Basu, A.R., Wang, J.W., Huang, W.K., Xie, G.H., Tatsumoto, M., 1991. Major element, REE, and Pb, Nd and Sr isotopic geochemistry of Cenozoic volcanic rocks of eastern China: implications for their origin from suboceanic-type mantle reservoirs. Earth and Planetary Science Letters 105, 149–169.

Brown, S.J.A., Fletcher, I.R., 1999. SHRIMP U–Pb dating of the pre-eruption growth history of zircons from the 340 ka Whakamaru Ignimbrite, New Zealand: evidence for >250 k.y. magma residence times. Geology 27, 1035–1038.

Chen, Y., Zhang, Y.X., Graham, D., Su, S.G., Deng, J.F., 2007. Geochemistry Cenozoic basalts and mantle xenoliths in Northeast China. Lithos 96, 108–126.

Condomines, M., 1997. Dating recent volcanic rocks through ^{230}Th–^{238}U disequilibrium in accessory minerals: Example of the Puy de Dome (French Massifc Central). Geology 25, 375–378.

Dunlap, C.E., Gill, J.B., Palacz, Z.A., 1992. U/Th disequilibria in the large-volume chemically-zoned eruption of Baitoushan, 1010 AD. EOS. Transactions of the American Geophysical Union 73, 611.

Fan, Q.C., Sui, J.L., Sun, Q., Li, L., Wang, T.H., 2005. Preliminary research of magma mixing and explosive mechanism of the Millennium eruption of Tianchi volcano. Acta Petrologica Sinica 21, 1703–1708.

Fan, Q.C., Sui, J.L., Wang, T.H., Li, L., Sun, Q., 2006. Eruption history and magma evolution of the trachybasalt in the Tianchi volcano, Changbaishan. Acta Petrologica Sinica 22, 1449–1457.

Fowler, S.J., Spera, F.J., 2007. Phase equilibria trigger for explosive volcanic eruptions. Geophysical Research Letters 35, L08309. doi:10.1029/2008GL033665.

Fu, B., Page, F.Z., Cavosie, A.J., Fournelle, J., Kita, N.T., Lackey, J.S., Wilde, S.A., Valley, J.W., 2008. Ti-in-zircon thermometry: applications and limitations. Contributions to Mineralogy and Petrology 156, 197–215.

Halliday, A.N., Mahood, G.A., Holden, P., Metz, J.M., Dempster, T.J., Davidson, J.P., 1989. Evidence for long residence times of rhyolitic magma in the Long Valley magmatic system: the isotopic record in precaldera lavas of Glass Mountain. Earth and Planetary Science Letters 94, 274–290.

Halliday, A.N., Davidson, J.D., Hildreth, W., Holden, P., 1991. Modelling the petrogenesis of high Rb/Sr silicic magmas. Chemical Geology 92, 107–114.

Harrison, T.M., Watson, E.B., Aikman, A.B., 2007. Temperature spectra of zircon crystallization in plutonic rocks. Geology 35, 635–638.

Hawkesworth, C.J., George, R., Turner, S., Zellmer, G., 2004. Time scales of magmatic processes. Earth and Planetary Science Letters 218, 1–16.

Hayden, L.A., Watson, E.B., 2007. Rutile saturation in hydrous silicious melts and its bearing on Ti-thermometry of quartz and zircon. Earth and Planetary Science Letters 258, 561–568.

Horn, S., Schmincke, H.U., 2000. Volatile emission during the eruption of Baitoushan Volcano (China/North Korea) ca. 969 AD. Bulletin of Volcanology 61, 537–555.

Le Bas, M.J., Le Maitre, R.W., Streckeisen, A., Zanettin, B., 1986. A chemical classification of volcanic rocks based on the total alkali–silica diagram. Journal of Petrology 27, 745–750.

Lei, J.S., Zhao, D.P., 2005. P-wave tomography and origin of the Changbai intraplate volcano in Northeast Asia. Tectonophysics 397, 281–295.
Liu, R.X., Wei, H.Q., Li, J.T., 1998. The Latest Eruptions from the Tianchi Volcano, Changbaishan. Science Press, Beijing, p. 159 (in Chinese with English Abstract).
Lowenstein, J.B., Clynne, M.A., Bullen, T.B., 1997. Comagmatic A-type granophyre and rhyolite from the Alid Volcanic Center, Eritrea, Northeast Africa. Journal of Petrology 38, 1707–1721.
Ludwig, K.R., 2003. User's Manual for ISOPLOT 3.00: A Geochronological Toolkit for Microsoft Excel. Berkeley Geochronology Center Special Publication, 4. Berkeley, 70 pp.
Machida, H., Arai, F., 1983. Extensive ash falls in and around the Sea of Japan from large late Quaternary eruptions. Journal of Volcanology and Geothermal Research 18, 151–164.
Mahood, G.A., 1990. Second reply to comment of R. S. J. Sparks, H. E. Huppert and C. J. N. Wilson on "Evidence for long residence times of rhyolitic magma in the Long Valley magmatic system: the isotopic record in the precaldera lavas of Glass Mountain". Earth and Planetary Science Letters 99, 395–399.
Miller, C.F., Wark, D.A., 2008. Supervolcanoes and their explosive supereruptions. Elements 4, 11–16.
Miller, J.S., Matzel, J.E.P., Miller, C.F., Burgess, S.D., Miller, R.B., 2007. Zircon growth and recycling during the assembly of large, composite arc plutons. Journal of Volcanology and Geothermal Research 167, 282–299.
Min, K., Mundil, R., Renne, P.R., Ludwig, K.R., 2000. A test for systematic errors in ^{40}Ar/^{39}Ar geochronology through comparison with U–Pb analysis of a 1.1 Ga rhyolite. Geochimica et Cosmochimica Acta 64, 73–98.
Monteleone, B.D., Baldwin, S.L., Webb, L.E., Fitzgerald, P.G., Grove, M., Schmitt, A.K., 2007. Late Miocene–Pliocene eclogite facies metamorphism, D'Entrecasteaux Islands, SE Papua New Guinea. Journal of Metamorphic Geology 25, 245–265.
Nakamura, T., Okuno, M., Kimura, K., Mitsutani, T., Moriwaki, H., Ishizuka, Y., Kim, K.H., 2007. Application of ^{14}C wiggle-matching to support dendrochronological analysis in Japan. Tree-Ring Research 63, 37–46.
Paces, J.B., Miller, J.D., 1993. Precise U–Pb ages of Duluth complex and related mafic intrusions, northeastern Minnesota — geochronological insights to physical, petrogenetic, paleomagnetic, and tectonomagmatic processes associated with the 1.1 Ga midcontinent rift system. Journal of Geophysical Research 98, 13997–14013.
Parker, D.F., 1983. Origin of the trachyte-quartz trachyte-peralkalic rhyolite suite of the Oligocene Paisano volcano, Trans-pecos Texas. Bulletin of Geological Society of America 94, 614–629.
Pringle, M.S., McWilliams, M., Houghton, B.F., Lanphere, M.A., Wilson, C.J.N., 1992. 40Ar/39Ar dating of Quaternary feldspar: examples from the Taupo Volcanic Zone, New Zealand. Geology 20, 531–534.
Putirka, K.D., 2008. Thermometers and barometers for volcanic systems. In: Putirka, K.D., Tepley III, F.J. (Eds.), Minerals, Inclusions and Volcanic Processes. Reviews in Mineralogy and Geochemistry. Mineralogical Society of America, Chantilly, VA, pp. 61–120.
Pyle, D.M., Ivanovich, M., Sparkes, R.S.J., 1988. Magma-cumulate mixing identified by U–Th disequilibrium dating. Nature 331, 157–159.
Reid, M.R., Coath, C.D., 2000. In situ U–Pb ages of zircons from the Bishop Tuff: no evidence for long crystal residence times. Geology 28, 443–446.
Reid, M.R., Coath, C.D., Harrison, T.M., McKeegan, K.D., 1997. Prolonged residence times for the youngest rhyolites associated with Long Valley caldera: ion microprobe dating of young zircons. Earth and Planetary Science Letters 150, 27–38.
Scaillet, B., Macdonald, R., 2006. Experimental constraints on pre-eruption conditions of pantelleritic magmas: evidence from the Eburru complex, Kenya Rift. Lithos 91, 95–108.
Schmitt, A.K., 2006. Laacher See revisited: high-spatial-resolution zircon dating indicates rapid formation of a zoned magma chamber. Geology 34, 597–600.
Schmitt, A.K., Grove, M., Harrison, T.M., Lovera, O.M., Hulen, J., Waters, M., 2003. The Guysers-Cobb Mountain Magma System, California (part 1): U–Pb zircon ages of volcanic rocks, conditions of zircon crystallization and magma residence times. Geochimica et Cosmochimica Acta 67, 3423–3442.
Schmitt, A.K., Wetzel, F., Cooper, K.M., Zou, H.B., Worner, G., 2010. Magmatic longevity of Laacher See Volcano (Eifel, Germany) indicated by U–Th dating of intrusive carbonatites. Journal of Petrology 51. doi:10.1093/petrology/egq011.
Self, S., Blake, S., 2008. Consequences of explosive supereruption. Elements 4, 41–46.
Self, S., Gertisser, R., Thordarson, T., Rampino, M.R., Wolff, J.A., 2004. Magma volume, volatile emissions, and stratospheric aerosols from the 1815 eruption of Tambora. Geophysical Research Letters 31, L20608.
Shangguan, Z.G., Zheng, Y., Dong, J., 1997. Compositions of the escaped gases from the Tianchi volcanic geothermal area, Changbai Mountains. Science in China 40, 390–397.
Siebert, L., Simkin, T., 2002. Volcanoes of the World: An Illustrated Catalog of Holocene Volcanoes and Their Eruptions. Smithsonian Institution, Global Volcanism Program Digital Information Series, GVP-3.
Sigurdsson, H., Carey, S., 1989. Plinian and co-ignimbrite tephra fall from the 1815 eruption of Tembora volcano. Bulletin of Volcanology 51, 243–270.
Simon, J.I., Renne, P.R., Mundil, R., 2008. Implications of pre-eruptive magmatic histories of zircons for U–Pb geochronology of silicic extrusions. Earth and Planetary Science Letters 266, 182–194.
Smith, P.E., York, D., Chen, Y., Envensen, N.M., 1996. Single crystal ^{40}Ar–^{39}Ar dating of a Late Quaternary paroxysm on Kos Greece: concordance of terrestrial and marine ages. Geophysical Research Letters 23, 3047–3050.
Sparks, R.S.J., 1986. The dimensions and dynamics of volcanic eruption columns. Bulletin of Volcanology 48, 3–15.
Su, W., Zhang, M., Redfern, S.A.T., Gao, J., Klemd, R., 2009. OH in zoned amphiboles of eclogite from the Easrtern Tianshan, NW-China. International Journal of Earth Sciences 98, 1299–1309.
Tang, J., Deng, Q., Zhao, G., Bai, D., Jin, G., Li, W., Xuan, F., Zhan, Y., Li, G., Hong, F., Ma, M., Chen, F., 2001. Electric conductivity and magma chamber at the Tianchi Volcano area in Changbaishan Mountain. Seismology and Geology 23, 191–200.
Turner, S., Costa, F., 2007. Measuring timescales of magmatic evolution. Elements 3, 267–272.
van den Bogaard, P., Schimick, C., 1995. ^{40}Ar/^{39}Ar laser probe ages of Bishop Tuff quartz phenocrysts substantiate long-lived silicic magma chamber at Long Valley, United States. Geology 23, 759–762.
Watson, E.B., 1979. Zircon saturation in felsic liquids: experimental data and applications to trace element geochemistry. Contributions to Mineralogy and Petrology 70, 407–419.
Watson, E.B., Harrison, T.M., 2005. Zircon thermometer reversals minimum melting conditions on earliest Earth. Science 308, 841–844.
Watson, E.B., Wark, D.A., Thomas, J.B., 2006. Crystallization thermometers for zircon and rutile. Contributions to Mineralogy and Petrology 151, 413–433.
Wei, H., Sparks, R.S.J., Liu, R., Fan, Q., Wang, Y., Hong, H., Zhang, H., Chen, H., J., H., Dong, J., Zheng, Y., Pan, Y., 2003. Three active volcanoes in China and their hazards. Journal of Asian Earth Sciences 21, 515–526.
Wei, H.Q., Melnik, O., Liu, Y.S., Barmin, A., Sparks, R.S.J., 2006. Conduit modeling of magma flow dynamics: a case study on the eruptive processes at the Tianchi volcano. Acta Petrologica Sinica 22, 3007–3013.
Wei, H.Q., Wang, Y., Jin, J.Y., Gao, L., Yun, S.H., Jin, B.L., 2007. Timescale and evolution of the intracontinental Tianchi volcanic shield and ignimbrite-forming eruption, Changbaishan, Northeast China. Lithos 96, 315–324.
Wiedenbeck, M., Alle, P., Corfu, F., Griffin, W.l., Meier, M., Oberli, F., Vonquadt, A., Roddick, J.C., Speigel, W., 1995. 3 natural zircon standards for U–Th–Pb, Lu–Hf, trace-element and REE analyses. Geostandards Newsletter 19, 1–23.
Zhao, D.P., Tian, Y., Lei, J.S., Liu, L., Zheng, S.H., 2009a. Seismic image and origin of the Changbai intraplate volcano in East Asia: role of big mantle wedge above the stagnant Pacific slab. Physics of the Earth and Planetary Interiors 173, 197–206.
Zhao, Z.D., Mo, X.X., Dilek, Y., Niu, Y.L., DePaolo, D.J., Robinson, P., Zhu, D.C., Sun, C.G., Dong, G.C., Zhou, S., Luo, Z.H., Hou, Z.Q., 2009b. Geochemical and Sr–Nd–Pb–O isotopic compositions of the post-collisional ultrapotassic magmatism in SW Tibet: petrogenesis and implications for India intra-continental subduction beneath southern Tibet. Lithos 113, 190–212.
Zou, H.B., Reid, M.R., Liu, Y.S., Yao, Y.P., Xu, X.S., Fan, Q.C., 2003. Constraints on the origin of historic potassic basalts from northeast China by U–Th disequilibrium data. Chemical Geology 200, 189–201.
Zou, H.B., Fan, Q.C., Yao, Y.P., 2008. U–Th systematics of dispersed young volcanoes in NE China: asthenosphere upwelling caused by piling up and upward thickening of stagnant Pacific slab. Chemical Geology 255, 134–142.
Zou, H.B., Fan, Q.C., Schmitt, A.K., Sui, J.L., 2010. U–Th dating of zircons from Holocene potassic andesites (Maanshan volcano, Tengchong, SE Tibetan Plateau) by depth profiling: time scales and nature of magma storage. Lithos 118, 202–210.